A First Principle calculation of $CaMoN_3$ perovskites material

Hardik Dave[1], Mitesh Solanki[2], Aditya Vora[3]
[1,3]*Department of Physics, Gujarat University, Ahmedabad, Gujarat, India*
[2]*Department of crystal growth and theoretical physics, pandit Deendayal Petroleum University, Gandhinagar, Gujarat. India*

***Abstract* - In the framework of density functional theory, the electronic structure of nitrogen-based $CaMoN_3$ was calculated in QUANTUM ESSPRESSO. Currently, GGA-PBE was used to precisely reproduce the ground-state parameters, as well as electrical and phonon properties. a variety of crystals. the electronic wave function in periodic crystal and augmented charges were represented by plane waves with cut-off energies The Brillouin zone was integrated using mesh of k-points and the Monkhorst–Pack scheme. These convergence variables characterize the band structure and density of early described states. Density functional perturbation theory estimates phonon properties using the linear response method. And Elastics Constant calculation of $CaMoN_3$ nitrogenase perovskite material.**

INTRODUCTION

Many inorganic nitrides, which are significant technical materials[1], fall into one of two families: hexagonal main-group metal nitride semiconductors, as well as cubic transition-metal nitride semiconductors[2].superconductors, are a type of superconductor (TMNs). This experimental and theoretical research identifies a family of ternary $Mg_xTM_{1x}N$ (TM = Ti, Zr, Hf, etc.) compounds[3]. Nb nitrides that act as a bridge between these groups. Nonetheless, these materials having crystal forms generated from rocksalt that are comparable to binary TMNs[4], They have enormous semiconducting band structures and semiconducting band structures when viewed electrically. dielectric constants, and characteristics that are disorder-tunable [5].

In the last decade, there has been a surge of interest in semiconducting II-IV-N2 ternaries[4], which are structurally similar to III-N wurtzite compounds but include the main-group III3+ metal[6].substituted with metals from groups II2+ and IV4+ (for example, Instead of Ga^{3+}[7], use $Zn2^{+}$[8] and Ge^{4+}[9]. We recently extended this materials design idea to ternary nitrides. other main-group (for example, Sb^{5+} in Zn_2SbN_3[2] and TM (Mo^{6+} in Zn_2SbN_3. The elements $ZnMo_3N_4$ [2] in wurtzite-derived crystal formations. However, it is unclear if a comparable method might be applied.

The use of first-principle calculations within the context of density functional theory (DFT) [10] to the analysis of physical characteristics of materials has proven effective[11]. The geometric structure created in this study is optimized using total energy minimization calculations, and the Nitrogen-based $CaMoN_3$ is used. The system with the lowest free energy is chosen for electronic structure computation[12]. The connection between DFT calculations for the geometric structure, electronic structure, Density of State, Phonon Calculation, and Elastic Constant properties are used to examine. In this research article

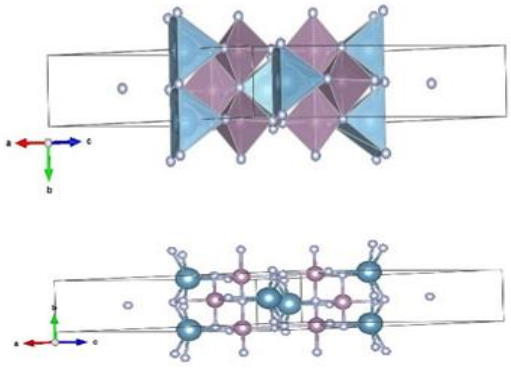

Figure 1. crystal structure of $CaMoN_3$ perovskite material

First Principle Calculation method

The extremely GGA pseudopotential approach was used to calculate the electronic structure of Nitrogen-

based $CaMoN_3$ in the context of density functional theory [13]. The QUANTUM ESSPRESSO we are using [14] In the current day within the context of generalized gradient approximation of Perdew-Burke-Ernzerhof (GGA-PBE) was used [15] which was discovered to perfectly replicate the ground state parameters, as well as electronic and phonon characteristics, are all included a diverse assortment of crystals Plane waves with cut-off energies as high as 60 Ry and 340 Ry was utilized to represent the electronic wave function in a periodic crystal [16] and enhanced charges, respectively. Over the Brillouin zone, integration was performed using a 999 mesh of k-points and the Scheme of Monkhorst–Pack [17]. These convergence factors are effective in characterizing the band structure and density of early investigation of [18] reported states based on the linear response method, the phonon characteristics are estimated using density functional perturbation theory[19]. The dynamical matrix, which gives information on lattice dynamics for the system, is produced using this approach. The dynamical matrix computations were carried out on a uniform grid of q-vectors in the Brillouin zone for a q-vector grid of 4 4 4 without the use of supercells [20] The above-mentioned kinetic energy cut-off and number of k-points result in phonon frequencies that converge in this system.

Electronic Structure Calculation:

At equilibrium, the electronic band structure and total density of states (TDOS) of the $CaMoN_3$ have been computed. Fig. 2 depicts the value of lattice constants. a, b, c, etc within the electronic band structure of the Fermi level is not spited in $CaMoN_3$.via indirect bandgap and separating L–V high symmetry the Brillouin zone's points There is, however, a zero. a gap in the band's structure.

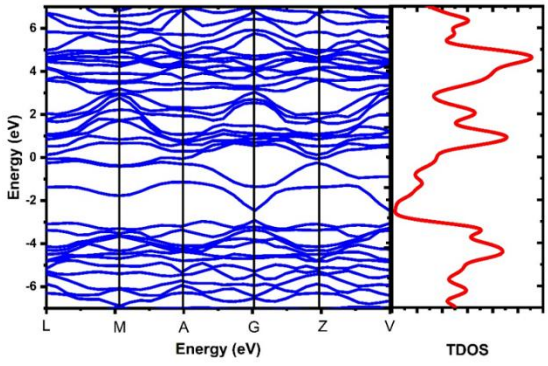

Figure 2 Electronic Band Structure of CaMoN3 perovskite crystals

Density of State:

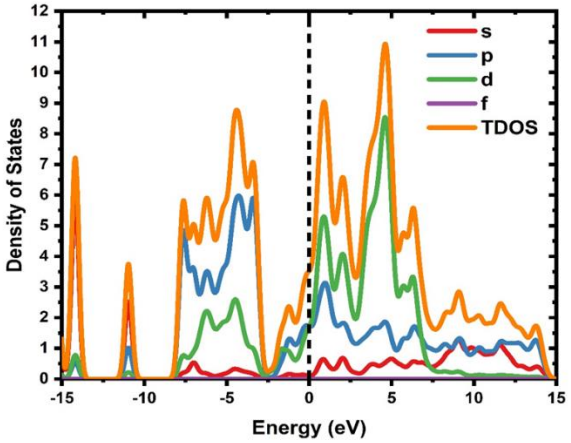

Figure 3 Partial Density of States of CaMoN3 perovskite crystals

The total and partial density of states of $CaMoN_3$ shown in Fig. 3 demonstrate that the valence band is made up of $CaMoN_3$ 2s, 3p, and d orbitals. The valence band's major contribution is related to the bonding hybridization between p and d of as well as bonding between 3d of copper and 3p of oxygen the main peaks in the valence band are caused by hybridized bonding orbitals. The conduction band, on the other hand, is mostly comprised of antibonding between (Ca) 2pand Mo (3d) orbitals have a minimal contribution to the conduction band minimum (CBM) (Fig. 3.)

Phonon Dispersive curve:

For $CaMoN_3$, the phonon dispersion curves (PDC) and phonon density of states (PDS) are shown in Fig.4.presented. And $CaMoN_3$nitrogen perovskite forms to better understand phonon mode behavior. and the important significance they play in the dynamical stability of a certain structure is provided[21]. The computed complete PDCs are displayed, together with the Brillouin zone's major symmetry directions (BZ) [22]. The phonon dispersion was computed for the first time. density functional theory (DFT) framework curves for $CaMoN_3$ nitrogen perovskite structures The PWSCF was used to investigate the phonon vibrations of(Quantum espresso) application software[14].

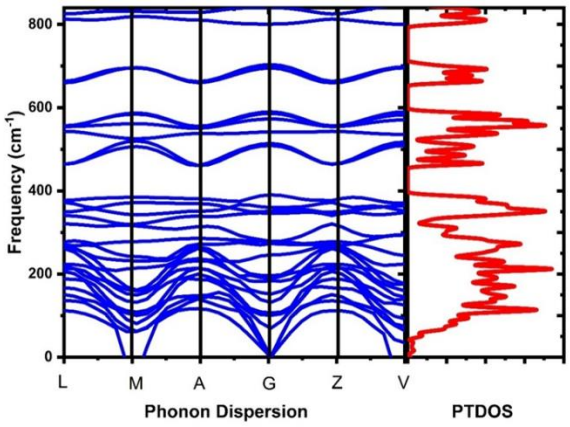

Figure 4. Phonon Dispersion Curve calculation in high symmetry point of CaMoN3 perovskite crystals

However, more band expanding $CaMoN_3$exhibits the same stable behavior in the crystal structure. An earlier work [23] reported on the vibrational frequencies of $CaMoN_3$ nitrogen perovskite is an extremely stable phonon dispersive spectral spectra [36]. additional band increasing and stable characteristics in the crystal structure are seen. In the paper, present Brillouin zone's L-V point, the L-V point acquired with the PBE-GGA(PWSCF) functional are utilizing this computation, as well as the phonon dispersion curves and high-symmetry directions of the Brillouin zone (BZ). where the contributions of various atoms and different phonon energy levels, Ca, Mo, And N are differentiated) phonon densities of states (DOSs) are calculated. the PWSCF phonon calculations Figure 4 depicts the total phonon DOSs. 7. In addition, the highest-frequency band of the $CaMoN_3$ nitrogen perovskite 0 to 800 cm^{-1}, while lst the lowest-frequency band cantered at 0 to 400 cm^{-1}. The stretching corresponds to 440 cm^{-1} of the $CaMoN_3$nitrogen perovskite system. Fig. 4 $CaMoN_3$ has five atoms, resulting in 25 vibrational phonon branches along with six high symmetric directions of the perovskite Brillouin zone of $CaMoN_3$structures, of which four are acoustic and five are optical. They have been seen at the U point of phonon dispersion curves and in the $CaMoN_3$ structure and no imaginary frequency was detected in any structure, but a high imaginary frequency was observed at the L, M, A, G, Z, and V locations. The phonon dispersion curves of the $CaMoN_3$perovskite structures are stable systems,

Elastic Constant:

The Bulk modulus (B) at the equilibrium value of lattice constant is calculated using the third-order Birch-Murunaghan equation of state [24].

$$E_V = E_0 + \frac{9BV_0}{16}\left\{\left[\left(\frac{V_0}{V}\right)^{\frac{2}{3}} - 1\right]^3 B' + \left[\left(\frac{V_0}{V}\right)^{\frac{2}{3}} - 1\right]^2 \times \left[6 - 4\left(\frac{V_0}{V}\right)^{\frac{2}{3}}\right]\right\} \quad \text{.....(1)}$$

Where V_0, V, Ev, B, and B' denote the atomic volume at P = 0 GPa, the atomic volume, the equilibrium energy at constant volume,

the bulk modulus, and the pressure derivative of the bulk modulus. Table 1 shows the equilibrium value of lattice constant and Bulk modulus for $CaMoN_3$perovskite phases, The value of bulk modulus (B) derived using the Birch-Murnaghan equation of state (EOS) is extremely similar to the value of bulk modulus (B0) obtained from the ElaStic code in Quantum espresso and is in good accord with previously reported results[25].

Structural	C11	C22	C33	C44	C55	C66	C12	C13	C23
$CaMoN_3$	58.09795	183.09270	14.32955	36.12325	8.10025	2.83545	46.44930	54.67885	36.69268

Table 1 Calculated elastic constants (Cij in GPa) for perovskite $CaMoN_3$ Crystals

Elastic constants are essential in determining mechanical and dynamical characteristics such as the equation of state, bulk modulus, and phonon spectra of a relaxed structure at zero pressure. Because the current structure is of the FCC type, there are three separate elastic elements.C11, C12, and C44 are constants required to indicate the elastic stability of a structure. The form of the structure varies with transverse strain at a given volume, whereas C11 changes with longitudinal strain. C12 and C44 are shear constants that indicate form elasticity [34]. Elastic constants may be used to relate different fundamental physical properties such as ductility. Brittleness, anisotropy, and elastic wave propagation in the material This data is accurate. Understanding the mechanical characteristics of the material is essential. Making use of elastic constants (Cij), The bulk modulus (B) and shear modulus (G) are calculated using the Voigt-Reuss-Hill method (VRH)[35-38] approximations

Furthermore, we can compute other significant parameters such as bulk modulus (B), Zenor anisotropy factor (A), Young's modulus (Y), Lam's constant () and (), Poisson's ratio (), and shear-modulus (G) using the following equations [29].

$A = \frac{2C_{44}}{(C_{11} - C_{12})}$.....(2)

$\mu = \frac{Y}{Y(1+\sigma)}$..... (3)

$\lambda = \frac{\sigma Y}{(1+2\sigma)(1-2\sigma)}$ ..... (4)

$Y = \frac{9GB}{(G+3B)}$…. (5)

$\sigma = \frac{\left(B-\frac{2}{3}G\right)}{\left(B+\frac{2}{3}G\right)}$…..(6)

Where $B = (C_{11} + 2C_{12})/3$ and $G = (G_V + G_B)/2$. The second and third terms are bulk modulus and isotropic shear modulus. respectively. 01 is the equivalent of Voigt's shear modulus or polycrystalline shear modulus. Gv is the top bound of G values, while Gr is the lower bound of G according to Reuss's shear modulus. values, which may be expressed as '01 percent $G_V = (C_{11} - C_{12} + 3C_{44})/3$and $\frac{5}{G_R} = \frac{4}{(C_{11}-C_{12})+ {}^{3}/_{C_{44}}}$calculated as a percentage The elastic constant values and the aforementioned parameters are mentioned in

The elastic constants (Cij) fulfill the elastic stability equation and demonstrate that the current structure is elastically and mechanically stable at the equilibrium value of the lattice constant. Table 2 shows the values of the elastic constant (Cij), the bulk modulus (B & B0), the Young modulus (Y), the Poisson ratio (P), the anisotropy factor (A), and the Cauchy's pressure (C11-C12). accord with results provided theoretically [18]. The Poisson's ratio is used to measure stability. of the material and informs on the nature of the bonding forces P's numerical value. It is modest for covalent materials (P = 0.1) and 0.25 for ionic materials.

Structural	B_V	B_R	B_H	G_V	G_R	G_H	Y	n
$CaMoN_3$	59.01798	17.27957	38.14878	17.25841	214.92725	116.09283	47.17668	0.36677

Table 2 Calculated bulk moduli (BV, BR, BH, in GPa), shear moduli (GV, GR, GH, in GPa), Young's moduli (Y, in GPa), and Poisson's ratio (n) for a perovskite $CaMoN_3$Crystals

The presence of a force in the solid is indicated by a value between 0.25 and 0.5 [34]. The ionic character of the compound is represented by P = 0.24 for Zr2MnAl. Cauchy's pressure is defined as C12 – C44 which denotes atomic bonding in metals and compounds Cauchy's negative values with directed bonding, pressure symbolizes the material's nonmetallic and brittle character. While a positive number indicates that the material is metallic and ductile [34], a negative value indicates that it is not metallic or ductile. Cauchy's pressure for Zr2MnAl is around 3.5 GPa, indicating the metallic and ductile character of the material. Anisotropic factor (A) is a physical number that represents the possibility of tiny fractures and voids forming in a material. A = 1 for an isotropic material and departure from this value measures the material's anisotropy [18]. In the event of A = 4.40 for Zr2MnAl, showing that the compound is anisotropic.

CONCLUSION

Semiconducting II-IV-N2 ternaries, which are structurally similar to III-N wurtzite compounds but include the main-group III3+ metal, have sparked a decade of research. This study's structure is optimized utilizing total energy minimization calculations, and the Nitrogen-based $CaMoN_3$ is utilized. The use of first-principle calculations within the framework of density functional theory (DFT) to the study of physical properties of materials has proved successful. The total and partial density of states of $CaMoN_3$. indicate that the valence band is composed of Ca MoN3 2s, 3p, and d orbitals. The main contribution of the Valence band is linked to bonding hybridization between p and d of as well as bonding between 3d of copper and 3p of oxygen. The conduction band, on the other hand, is mainly made up of antibonding between (Ca) 2p and Mo (3d) orbitals, with only a little contribution to the minimum (CBM) The third order Birch-Murunaghan equation of state is used to determine the Bulk modulus (B) at the equilibrium value of the lattice constant. C11, C12, and C44 are constants needed to show a structure's elastic stability. The structure's shape varies with transverse strain, while C11 varies with longitudinal strain. This data is correct since the present structure has three distinct elastic components. Bulk modulus and isotropic shear are the first two terms. The third word is the name of

the molecule type utilized in the research, which is referred to as Y or Y. The fourth term is a new word for where B = (C11 + 2C12)/3 and G = (GV + GB)/2. The fifth phase is derived from the Greek word for 'y,' which signifies "the number of atoms." Table 2 displays the elastic constant (Cij), bulk modulus (B & B0), Young modulus, Poisson ratio (P), and anisotropy factor values (A) Stability is measured using the Poisson's ratio. A positive score implies that the material is metallic and ductile, while a negative value indicates that it is neither metallic nor ductile. Cauchy's pressure is described as C12 – C44 in metals and compounds, which indicates atomic bonding.

REFERENCES

[1] A. Zakutayev, "Design of nitride semiconductors for solar energy conversion," *J. Mater. Chem. A*, vol. 4, no. 18, pp. 6742–6754, 2016, doi: 10.1039/c5ta09446a.

[2] D. Gogova *et al.*, "High electron mobility single-crystalline ZnSnN2on ZnO (0001) substrates," *CrystEngComm*, vol. 22, no. 38, pp. 6268–6274, 2020, doi: 10.1039/d0ce00861c.

[3] S. R. Bauers *et al.*, "Ternary nitride semiconductors in the rocksalt crystal structure," *Proc. Natl. Acad. Sci. U. S. A.*, vol. 116, no. 30, pp. 14829–14834, 2019, doi: 10.1073/pnas.1904926116.

[4] E. Arca *et al.*, "Redox-Mediated Stabilization in Zinc Molybdenum Nitrides," *J. Am. Chem. Soc.*, vol. 140, no. 12, pp. 4293–4301, 2018, doi: 10.1021/jacs.7b12861.

[5] B. G. Pfrommer, M. Cote, S. G. Louie, and M. L. Cohen, "Relaxation of crystals with the quasi-{N}ewton method," *J. Comput. Phys.*, vol. 131, pp. 233–240, 1997.

[6] H. Wang, H. Huang, and B. Wang, "First-principles study of structural, electronic, and optical properties of ZnSnO3," *Solid State Commun.*, vol. 149, no. 41–42, pp. 1849–1852, 2009, doi: 10.1016/j.ssc.2009.07.009.

[7] Z. Cui, K. Bai, X. Wang, E. Li, and J. Zheng, "Electronic, magnetism, and optical properties of transition metals adsorbed g-GaN," *Phys. E Low-Dimensional Syst. Nanostructures*, vol. 118, no. November 2019, p. 113871, 2020, doi: 10.1016/j.physe.2019.113871.

[8] F. Ye *et al.*, "Improving the chemical potential of nitrogen to tune the electron density and mobility of ZnSnN2," *J. Mater. Chem. C*, vol. 8, no. 13, pp. 4314–4320, 2020, doi: 10.1039/c9tc06965h.

[9] U. G. Jong, C. J. Yu, Y. H. Kye, Y. G. Choe, W. Hao, and S. Li, "First-Principles Study on Structural, Electronic, and Optical Properties of Inorganic Ge-Based Halide Perovskites," *Inorg. Chem.*, vol. 58, no. 7, pp. 4134–4140, 2019, doi: 10.1021/acs.inorgchem.8b03095.

[10] P. Giannozzi and S. Baroni, "Density-Functional Perturbation Theory," *Handb. Mater. Model.*, no. 2, pp. 189–208, 2005, doi: 10.1007/978-1-4020-3286-8_10.

[11] E. Gey, "Density-Functional Theory of Atoms and Molecules," *Zeitschrift für Phys. Chemie*, vol. 191, no. Part_2, pp. 277–278, 1995, doi: 10.1524/zpch.1995.191.part_2.277a.

[12] S. De Waele, K. Lejaeghere, M. Sluydts, and S. Cottenier, "Error estimates for density-functional theory predictions of surface energy and work function," *Phys. Rev. B*, vol. 235418, no. 23, pp. 1–13, 2016, doi: 10.1103/PhysRevB.94.235418.

[13] M. Bilal, S. Jalali-Asadabadi, R. Ahmad, and I. Ahmad, "Electronic properties of antiperovskite materials from state-of-the-art density functional theory," *J. Chem.*, vol. 2015, 2015, doi: 10.1155/2015/495131.

[14] P. Giannozzi *et al.*, "Q UANTUM ESPRESSO: a modular and open-source software project for quantum simulations of materials," vol. 395502, 2009, doi: 10.1088/0953-8984/21/39/395502.

[15] J. P. Perdew, K. Burke, and M. Ernzerhof, "Generalized Gradient Approximation Made Simple," *Phys. Rev. Lett.*, vol. VOLUME 77, no. 3, pp. 3865–3868, 1996, doi: 10.1103/PhysRevLett.77.3865.

[16] "Wave-Propagation-In-Periodic-Structures-Electric-Filters-And-Crystal-Lattices-First-Edition.pdf.".

[17] Hendrik J. Monkhorst, "Special points fro Brillouin-zone integretions," *Phys. Rev. B*, vol. 13, no. 12, pp. 5188–5192, 1976, doi: 10.1103/PhysRevB.13.5188.

[18] D. J. Chadi and M. L. Cohen, "Special points in the brillouin zone," *Phys. Rev. B*, vol. 8, no. 12, pp. 5747–5753, 1973, doi: 10.1103/PhysRevB.8.5747.

[19] S. Baroni, S. De Gironcoli, A. Dal Corso, and P. Giannozzi, "Phonons and related crystal properties from density-functional perturbation theory," *Rev. Mod. Phys.*, vol. 73, no. 2, pp. 515–562, 2001, doi: 10.1103/RevModPhys.73.515.

[20] S. Baroni, S. De Gironcoli, A. Dal Corso, and P. Giannozzi, "Phonons and related crystal properties from density-functional perturbation theory," *Rev. Mod. Phys.*, vol. 73, no. 2, pp. 515–562, 2001, doi: 10.1103/RevModPhys.73.515.

[21] C. Mno, "Journal of Magnetism and Magnetic Materials," vol. 332, pp. 61–66, 2013.

[22] M. Sato and Y. Ando, "Topological superconductors: A review," *Reports Prog. Phys.*, vol. 80, no. 7, pp. 1–45, 2017, doi: 10.1088/1361-6633/aa6ac7.

[23] L. Chang *et al.*, "Perovskite-type CaMnO3 anode material for highly efficient and stable lithium ion storage," *J. Colloid Interface Sci.*, vol. 584, pp. 698–705, 2021, doi: 10.1016/j.jcis.2020.04.014.

[24] F. Birch, "Finite elastic strain of cubic crystals," *Phys. Rev.*, vol. 71, no. 11, pp. 809–824, 1947, doi: 10.1103/PhysRev.71.809.

[25] M. B. Solanki, P. Pratik, S. Satyam, P. B. B, and J. Mihir, "Growth and characterization of lithium chloride doped KDP crystals: a DFT and experimental approach," *Ferroelectrics*, vol. 0, no. 0, pp. 1–16, doi: 10.1080/00150193.2020.1853734.